White Dwarf Stars

Adela Kawka

May 2, 2007

1 Introduction

White dwarf stars are the end products of stellar evolution for the majority of stars. After a star leaves the main-sequence it loses most of its mass to the surroundings leaving behind a hot dense core. This core which has ceased nuclear reactions. Therefore the core collapses under its own gravity until it becomes dense enough for the electrons to become degenerate producing enough pressure to prevent the core from collapsing any further. This is the beginning of star's final phase of evolution as a white dwarf. Since there are no more nuclear reaction the white dwarf simply cools down from a temperature of $\sim 100\,000$ K down to ~ 1000 K in about 10^{10} years.

2 History

The first star to be considered a white dwarf is the companion to the bright A star, Sirius. The mathematician, Friedrich W. Bessell observed Sirius between 1834 and 1844, and combined with previous observations dating back to 1755, noticed that Sirius was oscillating about its apparent path across the sky and concluded that it must have a companion (Bessell, 1844)[1]. For many years the companion remained unseen until 1862 when Alvan G. Clark, a son of an american telescope maker, visually detected the faint companion. He was testing his father's new 18-inch refractor and observed Sirius B at its predicted location[2] Shortly following this discovery, Bessel's predicted 50 year period of the system was confirmed. Due to the close proximity of Sirius B to Sirius B and Sirius A being 9 magnitudes brighter than its companion, Sirius B was not the first white dwarf to have its spectrum observed.

The first white dwarf to have its spectrum taken was 40 Eridani B (40 Eri B) as part the Henry-Draper Catalogue (Cannon & Pickering, 1918). Henry Norris Russell plotted the absolute magnitude versus the spectral type and noted the outstanding point in the plot. Figure 3 shows the original plot of H.R. Russell (Russell, 1914). The outstanding point is 40 Eri B which classified an A star, but

---

[1] At the same time he noticed that Procyon was showing the same behavior.

[2] Procyon B was first observed in 1986 by John M. Schaeberle using the 36-inch telescope at Lick Observatory.

H.N. Russell disregarded this because its "spectrum is very doubtful" (Russell, 1913). [3] In the same year Walter S. Adams noted its peculiarity (Adams, 1914).

The first spectrum of Sirius B was obtained in 1914 by Walter S. Adams using the 60-inch telescope at Mt. Wilson Observatory (Adams, 1915). As a result he gave Sirius B the classification of an A-type star, same as 40 Eridani B, the only other known white dwarf at that time. Adams (1925) obtained a second spectrum using the 100-inch telescope and used it to measure a gravitational redshift of 21 km s^{-1} (Adams, 1925), which was in agreement with Arthur S. Eddington's predicted value of 20 km s^{-1} (Eddington, 1924). Note, that even though Eddington has taken into account general relativity to calculate the gravitational redshift, Eddington assumed a structure for the white dwarf was wrong.

In 1926, Enrico Fermi and Paul Dirac showed that electrons obey what is now called the Fermi-Dirac statistics, which take into account the Pauli exclusion principle. And in the same year Ralph H. Fowler (Fowler, 1926) applied this new rule to white dwarf stars and showed that the pressure supporting white dwarfs against gravity is the electron degenerate pressure. Taking this theory further Subrahmanyan Chandrasekhar extended Fowler's work by including general relativity in the calculations and showed that there exists an upper limit on the mass of a white dwarf (Chandrasekhar, 1935). The derivation of the white dwarf structure is discussed in more detail in § 6.

When Chandrasekhar's structure for a white dwarf is adopted, a mass of 1.0 $M_\odot$ for Sirius B results in a radius of 0.008 $R_\odot$. The gravitational redshift can be calculated using:

$$\frac{v}{c} = \frac{\Delta\lambda}{\lambda} = \frac{GM}{c^2 R}$$

which results in $v_g = 78$ km s^{-1}, which is much larger than the value measured by Adams. A new gravitational redshift of 89 ± 16 km s^{-1} was obtained in 1971 by Greenstein et al.. This value is now in agreement with the predicted value, so why did Adams obtain a value that is so low? Wesemael (1985) showed that Adams' spectrum was heavily contaminated by Sirius A.

The most recent spectrum of Sirius B was obtained using the Hubble Space Telescope (Barstow et al., 2005). Figure 1 shows this spectrum and a gravitational redshift determined from this spectrum is 80 ± 5 km s^{-1}. Table 1 summarizes the properties of the Sirius system.

2.1 Proper Motion

The third white dwarf (van Maanen 2, WD 0046+051) was discovered in 1917 by Adriaan van Maanen during a search for stars with large proper motion (van Maanen, 1917). The proper motion of van Manaan 2 is 3" yr^{-1}. This is the first DZ white dwarf to be discovered. The discovery rate of white dwarfs increased

---

[3]In fact, H. R. Russell came across this star much earlier during his visit to the Harvard Observatory, where he discussed 40 Eri B with Edward M. Pickering. H.N. Russell asked about the spectral type of 40 Eri B which was of spectral class A. As a result, E.M. Pickering said "It is such discrepancies which lead to the increase of our knowledge."
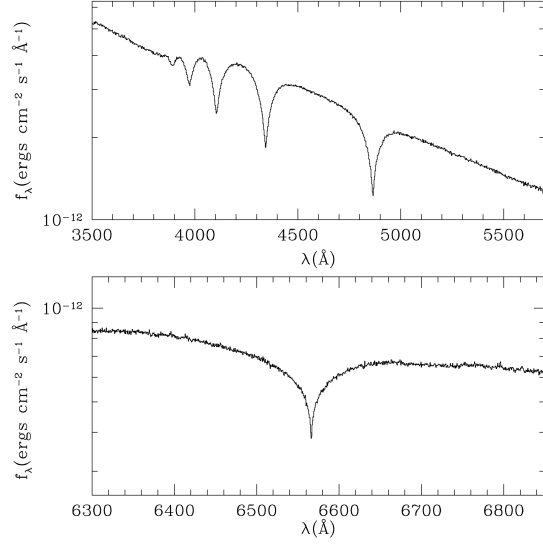
Figure 1: *HST* spectrum of Sirius B

Table 1: Properties of Sirius.

Parameter	Measurement	
Distance	2.63 pc	
Orbital Period	49.9 years	
	Sirius A	Sirius B
Apparent V magnitude	-1.5	8.0
Spectral Type	A1V	DA
Effective Temperature	9900 K	25 000 K
Mass	2.02 $M_\odot$	1.02 $M_\odot$
Radius	1.71 $R_\odot$	0.008 $R_\odot$
Gravitational redshift		80 ± 5 km s^{-1}

following the discovery of this star. By 1941, 38 white dwarfs were known (Kuiper, 1941). Willem J. Luyten conducted many proper motion surveys, which resulted in several catalogues:

- BPM: Bruce Proper Motion Survey

- LFT: Luyten Five-Tenths Catalog ($\mu \geq 0.5$" yr^{-1})

- LHS: Luyten Half-Second Survey ($\mu \geq 0.5$" yr^{-1})

- LTT: Luyten Two-Tenths Catalog ($\mu \geq 0.2$" yr^{-1})

- NLTT: New Luyten Two-Tenths Catalog ($\mu \geq 0.2$" yr^{-1})

In addition to measuring the stars proper motion, he also observed the stars in two photometric bands, red and blue which enabled him to distinguish between red and blue objects. In total W.J. Luyten observed more than $500\,000$ stars. Using the combination of the the photometry and proper-motion Luyten used the *reduced proper motion* diagram to classify the stars. The diagram is based on the idea that stars with large proper motion will be closer than stars with smaller proper motion, therefore the proper motion is a proxy for the distance of a star. The absolute magnitude (M) of a star with a known distance (d) in parsecs and apparent magnitude (m) is given by $M = 5 - 5\log d + m$. Therefore we can substitute the distance by the proper motion and simplify it to $m + \log \mu$ where μ is the proper-motion. A modern reduced proper-motion diagram is shown in Figure 2 which shows how the main-sequence, subdwarfs and white dwarfs can be distinguished (Salim & Gould, 2002).

Another major proper motion surveys that resulted in the discovery in many white dwarfs was the Lowell Proper Motion Survey (Giclas et al., 1971, 1978). Many white dwarfs were also discovered in colorimetric surveys that aimed at identifying objects with blue emission excess. A few of these surveys are

- Palomar-Green Survey (Green et al., 1986)

- Edinburgh-Cape (EC) Survey Kilkenny et al. (1997)

- Montreal-Cambridge-Tololo (MCT) Survey (Lamontagne et al., 2000)

- Hamburg/ESO (HE) Survey (Christlieb et al., 2001)

Hot white dwarfs are bright in the ultraviolet and as a result were detected by *International Ultraviolet Explorer* (*IUE*: e.g., Holberg et al. (2003)), the *Röntgen Satellite* (*ROSAT*: e.g., (Wolff et al., 1996; Marsh et al., 1997)) and the *Extreme Ultraviolet Explorer* (*EUVE*: Vennes et al. (1996, 1997)).

3   Evolution toward a white dwarf

About 90% of stars will evolve into white dwarfs. Stars with a mass of about 8 $M_\odot$ or less will eventually become a white dwarf, stars that are larger will
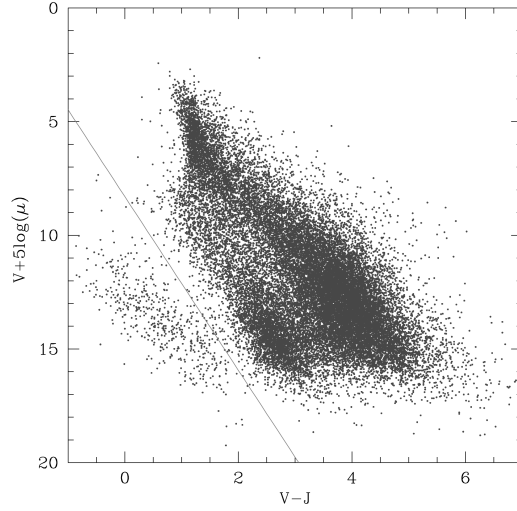
Figure 2: A Reduced Proper Motion diagram showing the grouping of revised NLTT objects grouped into main-sequence (top), subdwarfs (middle) and white dwarfs (bottom: below the demarcation line).
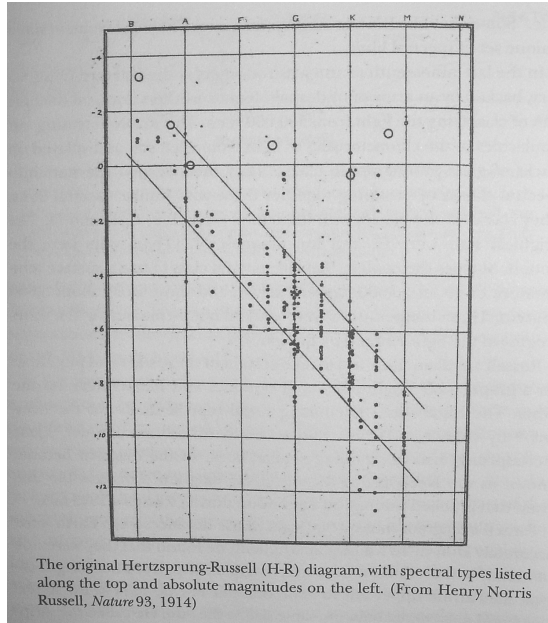

The original Hertzsprung-Russell (H-R) diagram, with spectral types listed along the top and absolute magnitudes on the left. (From Henry Norris Russell, *Nature* 93, 1914)

Figure 3: The original plot of Henry Norris Russell showing the absolute magnitude of stars versus their spectral type.
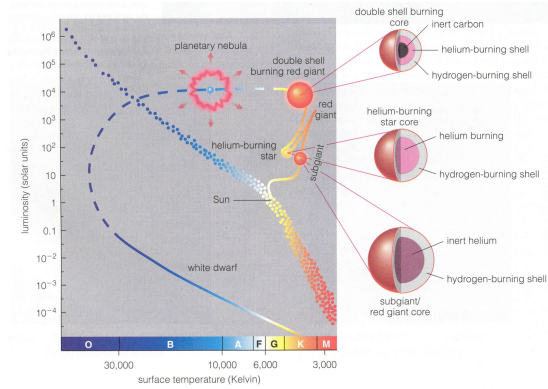
Figure 4: Hertzprung-Russell diagram showing the evolution of a 1 solar mass star after it leaves the main-sequence.

end their lives either as a neutron star or a black hole. An overview of how star like our Sun will become a white dwarf is summarized in Figure 4. The Sun will remain on the main-sequence for approximately 10 Gyrs during which it is burning H inside its core. When all the hydrogen is exhausted the core the Sun will move off the main-sequence and follow these steps:

1. Subgiant: the inert helium core will contract and hydrogen in the shell begins to burn.

2. Red giant: the helium core contracts until it becomes degenerate and it will ignite helium burning in a *Helium Flash*.

3. Horizontal branch (HB): at this stage we have helium burning in the core and hydrogen burning in the shell.

4. Asymptotic Giant Branch (AGB): a inert carbon/oxygen core but there is still helium and hydrogen shell burning.

5. Planetary nebula: ejection of the envelope due to super-wind.

6. White dwarfs.

4 Initial-to-final mass relations

The precise amount of matter lost during the planetary nebula stage is not known, but it does appear that stars of about 8 $M_\odot$ lose more than 80% of their mass to the planetary nebula. Young clusters where are turn-off at the main-sequence is observed are often used to help determine the initial to final mass relationship. In these clusters, the progenitor masses of the white dwarfs observed in the cluster have to be larger than the masses corresponding to the
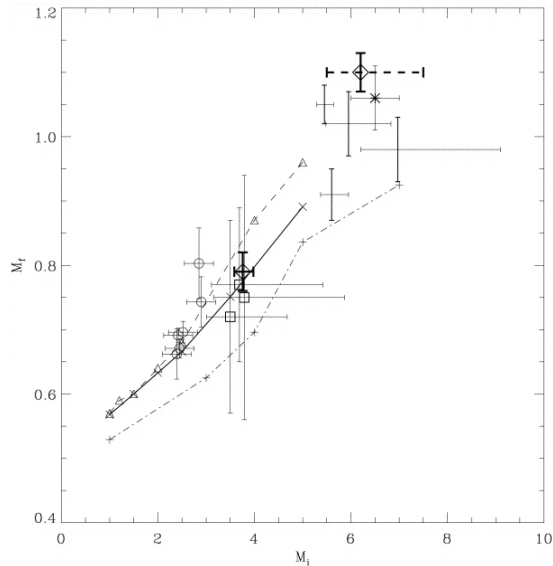
Figure 5: Empirical and theoretical M_i-M_f results. Diamonds with heavy error bars are for both members of PG 0922+162 (dashed error bars for PG 0922+162 B). The times symbol with error bars in upper right is result for Pleiad LB 1497. Points with thick error bars and without symbols, in upper right, are results for NGC 2516. Squares are results for NGC 3532. Circles are results for Hyades white dwarfs. The lines are for various theoretical relations (see Finley & Koester (1997)).

turn-off point on the main-sequence. Another way to determine the initial to final mass relations is to use wide binaries. For example, Finley & Koester (1997) used a pair a young white dwarfs (PG 0922+162) for which they derived cooling times for both stars and showed how the difference in these times translates into differences for the initial masses. Figure 5 shows the result of their study compared to the initial-to-final masses determined from open cluster studies, and some theoretical relations.

5   White Dwarf Properties

White dwarfs are very compact objects with very high densities ($\sim 10^6 - 10^9$ g m^{-3}). And because they are very compact, they have small radii, $\sim 1\%$ of the Solar radius, which is roughly the radius of the Earth and therefore have very low luminosities.

The atmosphere of a white dwarf is less than 1/1000th of the stellar radius, and it is here that the observed spectral lines are formed. The spectral classes of white dwarfs are defined below (as per Sion et al. (1983)), where the D in each case indicates that it is a *degenerate* star:

DA stars are hydrogen-rich showing H lines.

DO stars are helium-rich showing He II lines.

DB stars are helium-rich showing He I lines.

DC stars are helium-rich which a continuous spectrum.

DQ stars are helium-rich showing carbon features that can be either atomic or molecular.

DZ stars are helium-rich and show metal lines, for example the most commonly detected metals are Ca, Na, Mg, and Fe.

Some white dwarfs display a combination of the above mentioned spectral features and therefore all need to be used. For example a white dwarf showing Balmer lines and Ca II lines would be classified a DAZ. Example spectra of representative of the different spectral types are shown in Figure 6
Additional classifications based on other secondary features are as follows:

H for magnetic white dwarfs that do show any detectable polarization.

P for polarized magnetic white dwarfs.

V for variable white dwarfs.

And finally to complete the classification, a temperature index can follow their spectral classification. This index is defined as $\theta = 50400/T_{\text{eff}}$. Therefore, a white dwarf showing Balmer lines with an effective temperature of 20 000 K will be classified DA2.5. The temperature index is not always provided.

The temperature of white dwarfs ranges from $\sim 100\,000$ K down to about 3000 K. A white dwarf would take approximately 10^{10} years cover this temperature range during its cooling lifetime. Therefore, the cooling age is a function of the temperature. Note that the cooling rate is also dependent on the mass of the white dwarf. Figure 7 shows a Hertzprung-Russell diagram where the temperature and absolute magnitudes of white dwarfs from different samples are compared to the cooling curves (Wood, 1995) at different masses. Note the ZZCeti stars around $\sim 12\,000$ K, which are the variable DA white dwarfs.

Most white dwarfs have a mass that is between 0.4 $M_\odot$ and 1.2 $M_\odot$ with an average mass of 0.6 $M_\odot$. Figure 8 shows the mass distribution of a typical sample of non-magnetic white dwarfs compared to the mass distribution of magnetic white dwarfs. Note that the mass of magnetic white dwarfs appear to be systematically higher than that of non-magnetic white dwarfs. This can either be that magnetic white dwarfs evolve from more massive stars or the magnetic field (if it is fossil) caused mass to be retained during the planetary nebula stage. White dwarfs below ~ 0.4 $M_\odot$ most like formed in binary systems where there was some interaction with the companion, since the Galaxy is not old enough for these objects to have formed through single star evolution, i.e., the low-mass main-sequence stars have not had enough time to evolve of the main-sequence.
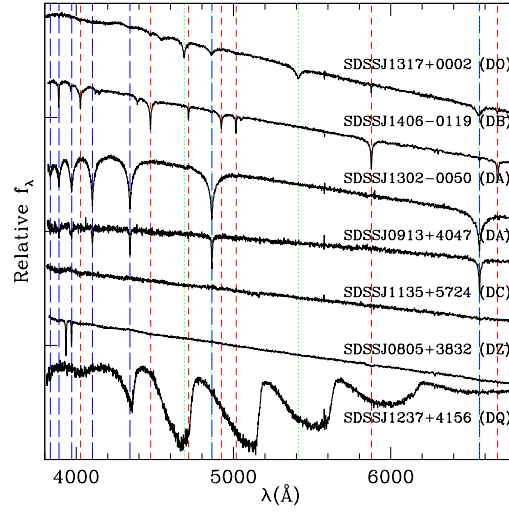
Figure 6: Example Sloan Digital Sky Survey spectra of different white dwarf spectral types. The *blue long-dashed* lines show the position of Balmer lines, the *red short-dashed* lines of HeI lines and *green dotted* of He II lines. The two narrow lines in the DZ white dwarf (SDSSJ0805+3832) are CaII, and the deep broad bands in SDSSJ1237+4156 are molecular carbon bands.
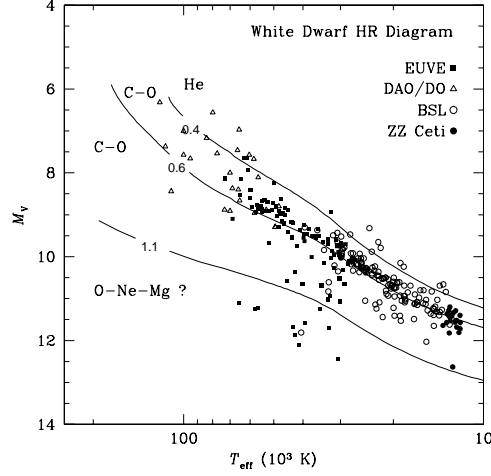
Figure 7: HR diagram showing white dwarfs from different samples compared to different cooling curves at 0.4 $M_\odot$, 0.6 $M_\odot$ and 1.1 $M_\odot$. The EUVE sample are hot white dwarfs selected that were detected by the Extreme Ultraviolet Explorer, the DAO/DO are hot white dwarfs showing HeII lines, the BSL are cooler white dwarfs observed by Bergeron et al. (1992) and ZZCeti sample are white dwarfs that are variable.
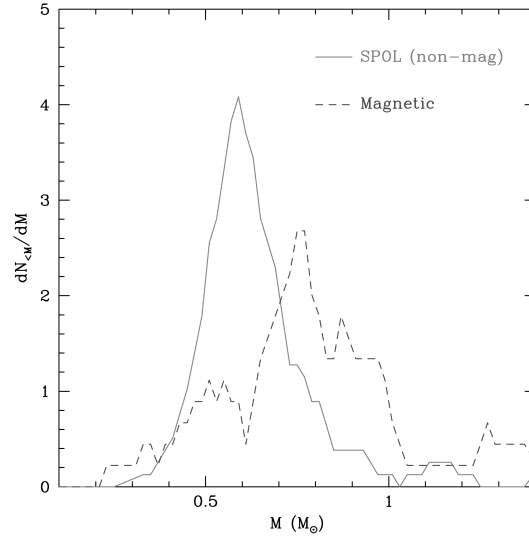

Figure 8: The mass distribution of a non-magnetic sample of white dwarfs (from Kawka et al., 2006) compared to the mass distribution of magnetic white dwarfs.
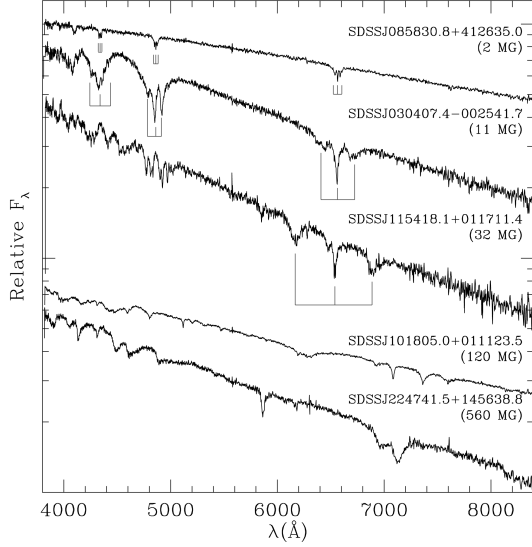
Figure 9: SDSS spectra of magnetic white dwarfs with magnetic fields showing the effect of the magnetic field strength on the hydrogen lines.

As already mentioned in the previous paragraph many white dwarfs show the presence of a magnetic field. About 20% of white dwarfs in the Solar neighborhood have magnetic fields that range from ~ 1 kG up to about 1000 MG. Compare this to the global magnetic field of the Sun which is about 1 G and the magnetic field strength near sunspots which have $B \sim 1 - 10$ kG.

The progenitors of magnetic white dwarfs are believed to be chemically peculiar Ap and Bp stars which harbor magnetic fields between ~ 1 kG and ~ 10 kG. Normal A and B stars appear to have weak magnetics, $B < 1$ G. If we assumed that magnetic flux is conserved during the final stages of evolution ($BR^2 = $ constant then the $1 - 10$ kG range for Ap/Bp stars would correspond to $\sim 10 - 100$ MG. This would explain the strongly magnetic white dwarfs. The white dwarfs with magnetic fields 1MG could evolve from less massive stars like our Sun.

White dwarfs are generally slow rotators, with rotational velocities less than 40 km s^{-1}. The rotation rates ($v \sin i$) cannot be measured using the broad Balmer lines, however they can be measured using the narrow hydrogen line cores. The rotation rates can also be measured using magnetic white dwarfs which are polarized. The polarization will vary as the white dwarf rotates (unless the white dwarf is inclined at either $i = 0°$ or $90°$). Another way to measure rotation rates is using astroseismology. This can be done with the special classes of variable white dwarfs, such as ZZ Cetis.

6 White dwarf structure

In 1926, Fermi and Dirac showed that electrons obey what is now called Fermi-Dirac statistics, which take into account the Pauli exclusion principle. Ralph H. Fowler applied this new rule to show that the pressure supporting white dwarfs against gravity is degenerate electron pressure. For a non-relativistic degenerate electron gas, the pressure is:

$$P_e = \frac{h^2}{5m} \left(\frac{3}{8\pi}\right)^{\frac{2}{3}} \left(\frac{\rho}{\mu_e M_\mu}\right)^{\frac{5}{3}} \tag{1}$$

where h is the Planck constant, m is the electron mass (9.11×10^{-28} g), ρ is the density, μ_e is mean electron molecular weight and M_μ is the atomic mass unit (1.66×10^{-24} g). Examining the above equation, we find that the pressure as a function of the density is a polytrope of index 3/2.

$$P = K \; \rho^{(n+1)/n} \tag{2}$$

For a fully relativistic and fully-degenerate electron gas, the pressure is:

$$P_e = \frac{ch}{8} \left(\frac{3}{\pi}\right)^{\frac{1}{3}} \left(\frac{\rho}{\mu_e M_\mu}\right)^{\frac{4}{3}} \tag{3}$$

where c is speed of light. This equation corresponds to a polytrope of index 3.

The mass-radius relationship of a white dwarf can be understood by a assuming a uniform density throughout the star, that is $\rho = M/(\frac{4}{3}\pi R^3)$ where M is the mass of the star and R is the stellar radius. The pressure P_c at the center of a star equals the weight per unit area of the material on top:

$$P_c = \frac{Mg}{A} = \frac{M}{4\pi R^2} \frac{GM}{R^2} = \frac{GM^2}{4\pi R^4} \tag{4}$$

Where g is the gravitational acceleration and G is the gravitational constant (6.673×10^{-34} Js). And in a white dwarf it is the degenerate electron pressure that prevents the star collapsing on itself, i.e., $P_c = P_e$. Assuming that the electron gas is non-relativistic (i.e., $P \propto \rho^{5/3}$), then:

$$\frac{M^2}{R^4} \propto \left(\frac{M}{R^3}\right)^{5/3}$$

$$\frac{M^2}{R^4} \propto \frac{M^{5/3}}{R^5}$$

$$R \propto M^{-1/3}$$

This relationship shows that the radius decreases as a function of an increasing mass. However, the density of a white dwarf is not uniform throughout its volume and also for white dwarfs that are more massive, the large gravities compress the mass into such high internal densities, that the electrons would

gain very high momenta and hence velocities that begin to approach the speed of light. Under these conditions it is necessary to adopt the fully relativistic and degenerate equation for the pressure of the electron gas ($P_e \propto \rho^{4/3}$).

To determine the structure of a star, we require that the star is in a hydrostatic equilibrium:

$$\frac{dP}{dr} = -\rho\, g = -\rho\frac{G\,M(r)}{r^2} \tag{5}$$

where $M(r)$ is the mass of the star at radius r. We also require the equation of mass continuity which ensures mass conservation.

$$\frac{M(r)}{dr} = 4\pi r^2 \rho \tag{6}$$

To solve the structure of a white dwarf, we need to combine the mass continuity (Eqn. 6) and the hydrostatic equilibrium (Eqn. 5) equations. Equation 5 can be re-written as:

$$\frac{r^2}{\rho}\frac{dP}{dr} = -GM(r)$$

and differentiating both side with respect to r, we get:

$$\frac{d}{dr}\left(\frac{r^2}{\rho}\frac{dP}{dr}\right) = -G\frac{dM(r)}{dr}$$

Here, we can insert the mass continuity equation:

$$\frac{d}{dr}\left(\frac{r^2}{\rho}\frac{dP}{dr}\right) = -G\;4\pi r^2 \rho$$

$$\frac{1}{r^2}\frac{d}{dr}\left(\frac{r^2}{\rho}\frac{dP}{dr}\right) = -4\pi G \rho \tag{7}$$

Lane and Emden suggested that a family of solutions may be obtained if one assumes that the pressure as a function of the density is a polytropic function (Eqn.2). Equations 1 and 3 are polytropes of indices $n = 3/2$ and 3, respectively.

To solve the Lane-Emden (L.E.) equation, we first scale ρ:

$$\rho = \lambda \Phi^n \tag{8}$$

where λ is a scaling factor. The pressure becomes:

$$P = K(\lambda\Phi^n)^{(n+1)/n} = K\lambda^{(n+1)/n}\Phi^{n+1}$$

which we substitute into the L.E. equation (Eqn. 7).

$$\frac{1}{r^2}\frac{d}{dr}\left(\frac{r^2}{\lambda\Phi^n}\frac{d(K\lambda^{(n+1)/n}\Phi^{n+1})}{dr}\right) = -4\pi G\lambda\Phi^n$$

$$\frac{1}{r^2}\frac{d}{dr}\left(\frac{r^2}{\lambda\Phi^n}K\lambda^{(n+1)/n}(n+1)\Phi^n\frac{d\Phi}{dr}\right) = -4\pi G\lambda\Phi^n$$

13

which when simplified results in:

$$\frac{K\lambda^{(1-n)/n}(n+1)}{4\pi G}\frac{1}{r^2}\frac{d}{dr}\left(r^2\frac{d\Phi}{dr}\right) = -\Phi^n \tag{9}$$

Here, we can define the "length" a:

$$a^2 = \frac{K\lambda^{(1-n)/n}(n+1)}{4\pi G} \tag{10}$$

and when substituted into Equation 9 we get:

$$\frac{a^2}{r^2}\frac{d}{dr}\left(r^2\frac{d\Phi}{dr}\right) = -\Phi^n \tag{11}$$

Finally we define a dimensionless scaling factor, $\xi = r/a$, and the L.E. equation becomes:

$$\frac{1}{\xi^2}\frac{d}{d\xi}\left(\xi^2\frac{d\Phi}{d\xi}\right) = -\Phi^n \tag{12}$$

At this point we can define the boundary conditions. At the center of the star ($\xi = 0$ and hence $r = 0$), the scaling factor $\lambda = \rho_c$ will be the central density and $\Phi = 1$, i.e., $\Phi = 1$ and $\rho = \lambda\Phi^n = \rho_c$ at $\xi = 0$. Rearrange, Equation 12 and differentiate:

$$\frac{d}{d\xi}\left(\xi^2\frac{d\Phi}{d\xi}\right) = -\Phi^n\xi^2$$

$$2\xi\frac{d\Phi}{d\xi} + \xi^2\frac{d^2\Phi}{d\xi^2} = -\Phi^n\xi^2$$

$$2\frac{d\Phi}{d\xi} + \xi\frac{d^2\Phi}{d\xi^2} = -\Phi^n\xi$$

And evaluating at $\xi = 0$, we get:

$$\frac{d\Phi}{d\xi} = 0$$

which becomes the second boundary condition. Now with the zeroth and first derivatives at $\xi = 0$ we can integrate outward (e.g., using the Runge-Kutta) and evaluate these functions until we reach the first zero of Φ which corresponds to $\rho = 0$, that is the surface of the star, where

$$\Phi(\xi_1) = 0$$

and therefore the stellar radius will be:

$$R = a\xi_1 = \sqrt{\frac{(n+1)K\lambda^{(1-n)/n}}{4\pi G}}\,\xi_1 \tag{13}$$

To obtain the mass of the star we integrate the mass-continuity equation (Eqn. 6):

$$dM = 4\pi r^2\rho dr$$

into which we substitute for r and ρ:

$$dM = 4\pi(a\xi)^2(\lambda\Phi^n)ad\xi = 4\pi a^3\lambda\Phi^n\xi^2 d\xi \qquad (14)$$

and using the L.E. equation (i.e., Eqn. 12) which we rewrite as:

$$\Phi^n\xi^2 d\xi = -d\left(\xi^2\frac{d\Phi}{d\xi}\right)$$

We now substitute this equation into Eqn. 14 to get:

$$dM = -4\pi a^3\lambda d\left(\xi^2\frac{d\Phi}{d\xi}\right)$$

Which can now be integrated from $M(\xi = 0) = 0$ to $M(\xi)$:

$$M(\xi) = -4\pi a^3\lambda\xi^2\frac{d\Phi}{d\xi} \qquad (15)$$

And the total mass of the star will be:

$$M(R) = M(\xi_1)$$

Analytical solutions exist for $n = 0, 1, 5$, however values for $n = 3/2, 3$ are numerical.

Figure 10 shows the calculated structure of white dwarf with a total mass of $0.6\ M_\odot$, where the density and integrated mass are plotted as a function of the radius. The Runge-Kutta 4th order integration method was used with a central density of $\rho_c = 3.39 \times 10^6$ g cm^{-3} which one of the initial boundary conditions. In the calculation, the mean electron molecular weight needs to be defined, and for fully ionized He, C, N or O, $\mu_e = 2.0$, which is the value that was adopted. The intergration was conducted until the total mass was well converged and the radius of a $0.6\ M_\odot$ was found to be $0.0105\ R_\odot$.

Repeating the integration for different central densities and hence obtaining different masses, we can calculate the mass-radius relation for white dwarfs. Figure 11 shows the mass-radius relation for white dwarfs where we assume $\mu = 2.0$ and $\mu = 2.151$ (for fully ionized iron). These mass radius relations are also compared to the simple relation, where $R \propto M^{-1/3}$.

For a white dwarf star that has a fully relativistic and degenerate electron gas we defined the pressure in Equation 3, that is:

$$P_e = \frac{ch}{8}\left(\frac{3}{\pi}\right)^{\frac{1}{3}}\left(\frac{\rho}{\mu_e\ M_\mu}\right)^{\frac{4}{3}}$$

Also the definition for a in Equation 10, which for $n = 3$ becomes:

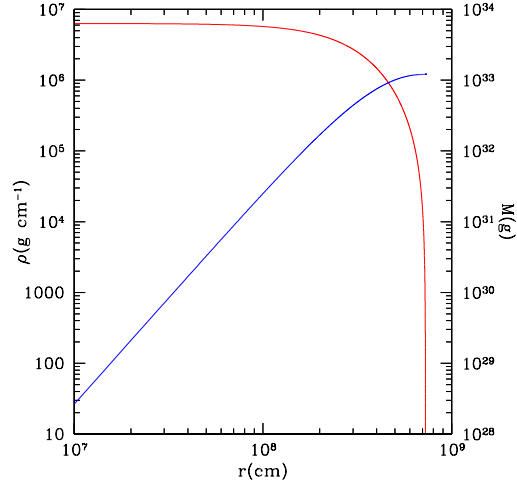$$a = \frac{1}{\lambda^{1/3}}\sqrt{\frac{K}{\pi G}}$$

15

Figure 10: The density and mass as a function of the radius of a white dwarf with a mass of 0.6 $M_\odot$.
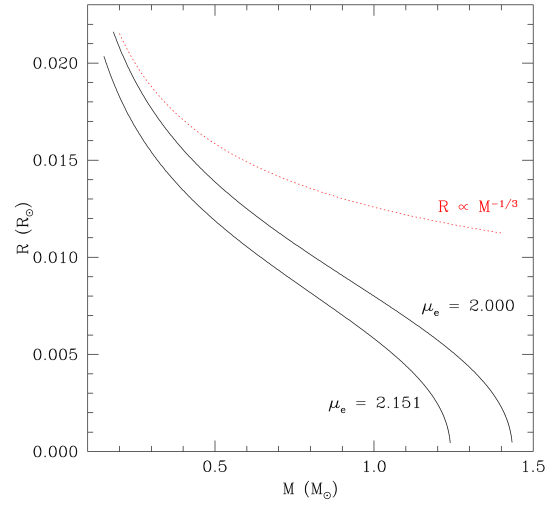

Figure 11: Mass-radius relations for white dwarfs.

16

which we can substitute into Equation 15 to get:

$$M(\xi) = -\frac{4}{\sqrt{\pi}}\left(\frac{K}{G}\right)^{3/2}\xi^2\frac{d\Phi}{d\xi} \qquad (16)$$

Remember that $P = K\rho^{(n+1)/n}$ and for $n = 3$ we get $P = K\rho^{4/3}$, therefore:

$$K = \frac{ch}{8}\left(\frac{3}{\pi}\right)^{1/3}\left(\frac{1}{\mu M_\mu}\right)^{4/3}$$

which we can substitute into Equation 16 to get:

$$M(\xi_1) = -\frac{4\sqrt{3}}{\pi}\left(\frac{hc}{8G}\right)^{3/2}\left(\frac{1}{\mu_e M_\mu}\right)^2\xi^2\frac{d\Phi}{d\xi} \qquad (17)$$

If we substitute for all constants and $-\xi_1^2(\frac{d\Phi}{d\xi})_{\xi_1} = 2.01824$ for $n = 3$, we find that the mass of the star is:

$$M = \frac{5.83}{\mu_e^2}M_\odot \qquad (18)$$

Therefore if every electron is relativistic then a single maximum mass is obtained, and this is known as the Chandrasekhar limit. And since most white dwarfs consist primarily of fully ionized helium, carbon and oxygen, then their electron molecular weight is $\mu_e = 2$, which reduces the above equation to:

$$M = 1.4M_\odot \qquad (19)$$

The mass-radius relations that we have considered are zero-temperature models, that is that they are independent of temperature. Note that the pressure of a completely degenerate electron gas is independent of its temperature. We observe surface temperatures, which imply that the white dwarfs are releasing energy and a temperature gradient exist within the star. This means that temperature needs to be included in the white dwarf model.

7 White Dwarf Cooling

Since no nuclear reactions occur in the interior of a white dwarf, then white dwarfs simply cool off as they slowly release their supply of thermal energy. It is necessary to understand the rate at which a white dwarf cools so that its age can be determined. This is very useful in understanding the history of star formation in our Galaxy.

In ordinary stars, photons travel much further than atoms before they collide with an atom and lose their energy, and therefore are responsible for most of the energy transport inside the stellar interior. White dwarfs are very dense, and photons would travel very short distances before they collide with a nucleus and lose their energy. However, degenerate electrons can travel long distances before losing energy in a collision with a nucleus, since the majority of the lower-energy electron states are already occupied. Therefore in a white dwarf energy is transported via electron conduction which is more efficient than radiation.

The modern theory of white dwarf cooling was established by Mestel (1952) who showed that the white dwarf loses its thermal energy through the thin layer of non-degenerate atmosphere.

Since white dwarfs lack nuclear processes as an energy source, the evolution is simply driven by the rate of change of internal energy as heat is radiated out. From thermodynamics, the internal energy u is related to the entropy s of the system by $du = Tds$ (at constant volume and number of particles). Therefore the rate of energy dissipated as heat is:

$$\frac{du}{dt} = T\frac{ds}{dt} = T\left(\frac{\partial s}{\partial T}\right)_\rho \frac{\partial T}{\partial t} + T\left(\frac{\partial s}{\partial \rho}\right)_T \frac{\partial \rho}{\partial t} \tag{20}$$

The specific heat of a gas at constant volume is simply $(\partial u/\partial T)_V$ and if we assume that there is no gravitational contraction (i.e., $\partial \rho/\partial t = 0$) then the above equation simplifies to:

$$\frac{du}{dt} = c_V \frac{\partial T}{\partial t} \tag{21}$$

In the interior of a white dwarf, the electrons are degenerate but the ions are non-degenerate. The heat capacity per unit volume c_V of a gas that consists of non-degenerate ions and non-relativistic electrons is:

$$c_V = \frac{3}{2}n_i k + \frac{\pi^2}{2}n_e k\left(\frac{kT}{E_F}\right) \tag{22}$$

where E_F is the Fermi energy, n_i and n_e are the number density of ions and electrons, respectively, k is the Boltzmann constant and T is the temperature of the gas. From the equation we can see that electrons do not contribute significantly to the heat capacity inside the white dwarf because the electrons are strongly degenerate (i.e., $E_F \gg kT$).

Since the luminosity of a white dwarf star is maintained by the thermal energy of ions, then the luminosity L is:

$$L = -\frac{dU}{dt} = -\frac{d}{dt}\int\int c_V\, dT\, dV \tag{23}$$

We also require a relationship between the core temperature and the surface temperature in order to calculate an evolutionary scenario. The interior of a white dwarf is isothermal due to the very high electron conductivity. The temperature change from the interior to the surface occurs within a thin layer of essentially non-degenerate gas. The energy transport through this layer is assumed to be due to radiative diffusion. The opacity κ of the gas in this layer is caused by free-free and bound-free absorption and can be expressed by Kramer's law:

$$\kappa = \kappa_0 \rho T^{-3.5} \tag{24}$$

where κ_0 is a constant that depends on the composition.

To derive the pressure as a function of the temperature in these layers, we need to combine the hydrostatic equilibrium equation (Equation 5) with the

equation for radiative transfer. In these layers, we assume that the mean free path of a photon is much less than the temperature scale height, and therefore the radiation is very close to that of a blackbody. Therefore the radiative transfer in these layers is:

$$\frac{L}{4\pi r^2} = -\frac{4ac}{3\rho\kappa}T^3\frac{dT}{dr} \tag{25}$$

where $a = 7.564 \times 10^{-15}$ erg cm^{-3} K^{-4}. We can rearrange the above equation such that:

$$dr = -\frac{4\pi r^2}{L}\frac{4ac}{3\rho\kappa}T^3 dT$$

which we substitute into the equation for hydrostatic equilibrium and obtain:

$$\frac{dP}{dT} = \frac{4ac}{3\kappa}\frac{4\pi GM}{L}T^3$$

and finally substituting in Kramer's law for opacity (Eqn. 24) and simplifying:

$$\frac{dP}{dT} = \frac{4ac}{3}\frac{4\pi GM}{L\rho\kappa_0}T^{6.5} \tag{26}$$

Close to the surface of the white dwarf, the gas is non-degenerate and the pressure can be approximated by the pressure for an ideal gas. Here we assume that the gas is fully ionized and the coulomb interaction energy is much less than the kinetic energy.

$$P_i = \frac{\rho kT}{\mu m_p} \tag{27}$$

where m_p is the mass of a proton, since we assume that the pressure is mostly provided by ionized hydrogen. We can now eliminate ρ from Equation 26 by substituting in Equation 27 to obtain:

$$PdP = \frac{4ac}{3}\frac{4\pi GMk}{L\kappa_0\mu m_p}T^{7.5}dT$$

Given that the photospheric temperature of the white dwarf is small compared to the interior temperature we can integrate the above equation with the boundary condition such that $T = 0$ at $P = 0$.

$$P^2 = \frac{2}{8.5}\frac{4\pi Gk}{\kappa_0\mu m_p}\frac{M}{L}T^{8.5}$$

Now we substitute for pressure using Equation 27 and simplifying:

$$\rho = \left(\frac{2}{8.5}\frac{4ac}{3}\frac{4\pi GM}{\kappa_0 L}\frac{\mu m_p}{k}\right)^{1/2}T^{3.25} \tag{28}$$

To simplify further calculations, we will define:

$$K_1 = \left(\frac{2}{8.5}\frac{4ac}{3}\frac{4\pi G}{\kappa_0}\frac{\mu m_p}{k}\right)^{1/2} \tag{29}$$

19

and therefore Equation 28 will become:

$$\rho = K_1 \left(\frac{M}{L}\right)^{1/2} T^{3.25} \tag{30}$$

This equation assumed a non-degenerate gas in its derivation, which becomes invalid at densities where electron degeneracy becomes important. At the boundary of the isothermal core with the outer non-degenerate envelope, we assume that the pressure of the non-degenerate electron gas is equal to the pressure of a completely degenerate electron gas (Eqn. 1) with a temperature of the isothermal core, T_c:

$$\frac{\rho_c k T_c}{\mu_e M_\mu} = \frac{h^2}{5m}\left(\frac{3}{8\pi}\right)^{\frac{2}{3}}\left(\frac{\rho_c}{\mu_e M_\mu}\right)^{\frac{5}{3}} \tag{31}$$

where ρ_c is the gas density at the core boundary. And rearranging to obtain the density at the core boundary:

$$\rho_c = \frac{8\pi}{3}\left(\frac{5mk}{h^2}\right)^{3/2} \mu_e M_\mu T_c^{3/2}$$

$$\rho_c = K_2 T_c^{3/2} \tag{32}$$

where

$$K_2 = \frac{8\pi}{3}\left(\frac{5mk}{h^2}\right)^{3/2} \mu_e M_\mu \tag{33}$$

And if we assume that Equation 30 is valid at the core boundary, i.e., $\rho = \rho_c$ and $T = T_c$, then:

$$K_1 \left(\frac{M}{L}\right)^{1/2} T_c^{3.25} = K_2 T_c^{3/2}$$

Solving for the luminosity to obtain:

$$L = \left(\frac{K_1}{K_2}\right)^2 M T_c^{3.5} \tag{34}$$

The available thermal energy of an isothermal white dwarf with a temperature T_c is provided mainly by the non-degenerate ions. The available thermal energy is:

$$U = \int c_V T dV = \int \frac{c_V}{\rho} dM \simeq \frac{\bar{c}_V}{\bar{\rho}} T_c M$$

where $\bar{c}_V$ and $\bar{\rho}$ are the mean values for the heat capacity c_V and density ρ. Comparing this to Equation 23:

$$L = -\frac{dU}{dt}$$

Combining this equation with Equation 34 and our approximation for the available thermal energy in a white dwarf star, we get

$$-\frac{dU}{dt} = \left(\frac{K_1}{K_2}\right)^2 M T_c^{3.5}$$

$$-\frac{d}{dt}\left(\frac{\bar{c}_V}{\bar{\rho}}T_c\right) = \left(\frac{K_1}{K_2}\right)^2 T^{3.5}$$

Note that the mass M cancels out, and if we assume that the average heat capacity $\bar{c}_V$ is time independent, then the integral of the above equation where the initial temperature T_0 occurs at some time t_0 is:

$$-d\left(\frac{\bar{c}_V T_c}{\bar{\rho}}\right) = \left(\frac{K_1}{K_2}\right)^2 T_c^{3.5} dt$$

$$-d\left(\frac{\bar{c}_V}{\bar{\rho}}\frac{1}{T_c^{2.5}}\right) = \left(\frac{K_1}{K_2}\right)^2 dt$$

$$\frac{2}{5}\frac{\bar{c}_V}{\bar{\rho}}\left(\frac{1}{T^{2.5}} - \frac{1}{T_0^{2.5}}\right) = \left(\frac{K_1}{K_2}\right)^2 (t - t_0) = \left(\frac{K_1}{K_2}\right)^2 \tau \tag{35}$$

If we assume that that $T \ll T_0$, then:

$$\tau = \frac{2}{5}\left(\frac{K_2}{K_2}\right)^2 \left(\frac{\bar{c}_V}{\bar{\rho}}\right)\frac{1}{T_c^{2.5}}$$

and substituting in Equation 34 we get the relationship:

$$\tau = \frac{2}{5}\left(\frac{\bar{c}_V}{\bar{\rho}}\right)\frac{T_c M}{L} \tag{36}$$

and again substituting in Equation 34, we can eliminate T_c and obtain:

$$\tau = \frac{2}{5}\frac{\bar{c}_V}{\bar{\rho}}\left(\frac{K_2}{K_1}\right)^{4/7}\left(\frac{M}{L}\right)^{5/7} \tag{37}$$

Here τ is the so called *cooling age*, that is the time required for the luminosity of a white dwarf to go from L_0 to L, where we have assumed L_0 to be very large compared to L when we assumed that $T \ll T_0$. Rearranging of the above equation and making the relevant substitutions for the mean density, mean specific heat, opacity, and constants, we can find the luminosity as a function of the cooling age:

$$L \approx 8.4 \times 10^{-4} L_\odot (M/M_\odot)\,\tau_9^{-7/5} \tag{38}$$

where τ_9 is the cooling age in 10^9 years.

This simple power-law cooling model shows the basics of how a white dwarf cools and it is a good approximation to more detailed cooling models. This is the simplest view of how white dwarfs cool. However, the cooling history of a white dwarf is more complex. And to construct a more representative model of white dwarf cooling we need to consider several more elements.

The above model only considers the release of thermal energy, however as a white dwarf cools there are additional energy sources that need to be considered. These will be briefly discussed below:
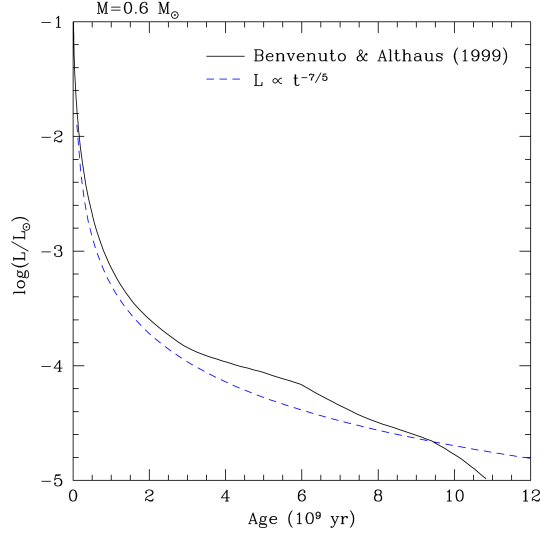
Figure 12: Theoretical cooling curves for a white dwarf with a mass of 0.6 $M_\odot$.

Gravitational energy: In our model we have assumed that there is no gravitational contraction, and therefore that there is no evolution in the hydrostatic structure. However, the star is losing thermal energy and it is actually shrinking, and therefore releasing gravitational energy, contributing to the energy loss.

Nuclear energy: The cooling age can be affected by any residual hydrogen burning on the surface of the white dwarf. When the progenitor of a white dwarf finally runs out of nuclear fuel to burn, the progenitor rapidly contracts into a white dwarf. Due to the strong gravity a diffusion of elements takes place, that is the heaviest elements will diffuse downwards and the lightest upwards. This may lead to a possible enhanced concentration of CNO and allow the CNO cycle to continue and reduce the hydrogen content in the atmosphere, which may explain why there are some hydrogen-poor white dwarfs.

Low-mass stars no helium-flash occurs, and therefore end up with thicker hydrogen layers, which may continue burning by the proton-proton process, and this additional burning can also prolong the cooling age of a white dwarf star.

Crystallization: In the white dwarf, the heat content is regulated by the ions, which can be described as positively charged nuclei at a particular density and temperature that are immersed in a sea of neutralizing degenerate electrons. Therefore, Coulomb interactions play an important part in how these ions behave.

A very young white dwarf is very hot and therefore the ions can be assumed

to behave like an ideal gas, however as it cools down, it will begin to crystallize from the center outwards. When this begins to occur, the ions are essentially changing phase, and therefore release latent heat during crystallization. This slows the white dwarf's cooling and can be observed as an upturned *bump* in the cooling curve. Figure 12 compares the cooling curve that was derived above (i.e., Eqn. 37) to a model cooling curve (Benvenuto & Althaus, 1999) that includes crystallization and other effects. Once the interior of the white dwarf has crystallized and the temperature continues to decrease, the crystalline structure accelerates the cooling. That is the vibration of the regularly spaced nuclei promotes energy loss. This can be observed in Figure 12 as the sharp downturn in the cooling curve.

The evolution of a white dwarf is not only determined by the available energy sources but also by the processes that transport the energy to the surface. The structure of a white dwarf can be separated into the core where the electrons are degenerate and the thin, non-degenerate envelope. Even though this envelope is very thin and its mass is a very small fraction of the white dwarfs total mass, it is here where the energy transport is slowest and hence determines the cooling rate.

We have already mentioned that it is electron conduction that is responsible for energy transport inside the white dwarf core. However, the early and hence hot stages of white dwarf evolution is dominated by neutrino losses. Neutrino luminosity is not dominant in the final stages of AGB evolution, however it is important, so when the white dwarf starts to collapse following the end of shell burning, the photon luminosity drops, but the neutrino luminosity does. Here the neutrino luminosity is driven by the central temperature of the white dwarf.

The energy transport in the thin, non-degenerate envelope can be either via radiative transport and/or convective energy transport for cooler white dwarfs. The temperature at which a convective zone develops depends on the composition of the thin non-degenerate envelope (atmosphere).

8 Model Atmospheres

The atmosphere of a star consists of the layers of the star that can be observed. The thickness of the atmosphere of a white dwarf does not exceed 1/1000th of a stellar radius in thickness ($h_{\mathrm{atmos}}/R_{\mathrm{star}} < 10^{-3}$) from which radiation escapes into the vacuum of space. We can model the atmosphere by solving a set of equations which will provide a physical description of the observable region of a star. Since the thickness of the atmosphere of a white dwarf is much smaller than the radius of the star, we can assume plane-parallel geometry, that is the geometry of the atmosphere is unidimensional and parametrized by the height z.

The radiated flux emitted at the surface of the star is frequency dependent and is expressed as the *Eddington* flux, $H_\nu(z = z_0)$, where z_0 indicates the surface, and carries the units erg cm^{-2} s^{-1} Hz^{-1} steradian^{-1}. The total flux

emitted by the star is given by integrating over all solid angles and frequencies:

$$\mathcal{F}_{\text{total}} = 4\pi H_{\text{total}} = 4\pi \int_0^\infty H_\nu d\nu = \sigma_R \, T_{\text{eff}}^4, \tag{39}$$

where $\sigma_R = 5.67 \times 10^{-5}$ erg cm^{-2} s^{-1} K^{-4} is the Stefan-Boltzmann constant, and the above equation defines T_{eff}, the effective temperature.

The atmosphere can modeled by solving a set of non-linear equations, which will provide a physical description of the observable region of the star:

- Energy transfer, which can be either or both radiative and convective.

- Radiative equilibrium, which implies energy conservation within the atmosphere. The energy that enters the atmosphere must be equal to the energy leaving the atmosphere, that is no energy is created or lost inside the atmosphere.

- Hydrostatic equilibrium, that is where the gas pressure balances the gravitational forces.

- Equation of state, that is the population of the energy levels.

- Charge and particle conservation, where the total number of particles is conserved and that the net electric charge is zero.

We solve the problem numerically, and therefore we first need to choose the independent variable. In this case, it is better to select the Lagrangian mass m, which is the mass as a function of the depth (i.e., mass loading), rather than the optical depth. The optical depth τ is defined as the probability that a photon will escape from a certain depth inside the star into space $e^{-\tau}$. Therefore the optical depth increases from the surface inward. The reason for using m simplifies the equation for hydrostatic equilibrium. And the optical depth is related to the thickness dz at depth z by:

$$d\tau = -\chi dz$$

however we wish to use the variable m in our calculations:

$$dm = -\rho dz$$

where ρ is the density of the atmosphere. Combining the two equations we get a relationship between the mass loading and the optical depth.

$$d\tau = \frac{\chi}{\rho} dm$$

Since the problem is being solved numerically, discrete variables need to be used. Therefore the atmosphere needs to be sliced into layers, and the spectrum into discrete frequencies. For example:

$$m \longrightarrow m_d \quad (d = 1, \text{ND})$$

$$T = T(m_d) \longrightarrow T_d \qquad (d = 1, \text{ND})$$

$$H_\nu \longrightarrow H_{d,j} \qquad (d = 1, \text{ND}; j = 1, \text{NJ})$$

We can now define the equations that will be used. The energy transport in white dwarfs is mostly radiative transfer:

$$\frac{\partial H_\nu}{\partial z} = \chi_\nu (S_\nu - J_\nu)$$

where J_ν is the specific intensity and S_ν is the source function and is defined by:

$$S_\nu = \frac{\eta_\nu}{\chi_\nu}$$

and η_ν is emissivity, and the equation represents the transfer of energy within a layer of the atmosphere dz taking into account absorption and emission at any given frequency. Integrating the radiative transfer equation over all frequencies leads to the radiative equilibrium that is the conservation of energy.

$$\frac{\partial H}{\partial z} = 0 = \int \chi_\nu (S_\nu - J_\nu) d\nu$$

When calculating the flux throughout the atmosphere a boundary condition needs to be defined. We need the total flux leaving the surface to be (i.e., the boundary condition):

$$\mathcal{F} = 4\pi H = 4\pi \int_0^\infty H_\nu d\nu = \sigma_R T_{\text{eff}}^4$$

We also need the atmosphere to be in hydrostatic equilibrium.

$$\frac{dP}{dz} = -\rho g \longrightarrow \frac{dP}{dm} = -g,$$

In the atmosphere we can assume that the particles follow the ideal gas law, and hence the pressure acting against gravitational contraction is:

$$PV = NkT \longrightarrow P = nkT$$

where N is the number of particles and therefore $n = N/V$ is the particle density.

The atmosphere needs to be in statistical equilibrium, where the ionization fractions are described the Saha equation:

$$\frac{n_i}{n_{i+1}} = \frac{u_i}{u_{i+1}} N_e \Phi(T)$$

where n and u are the number density and the partition function, respectively, of the ith and $i + 1$th ionization states, and $\Phi(T)$ for hydrogen is:

$$\Phi(T) = \left(\frac{h^2}{2\pi mkT} \right)^{3/2} e^{\chi_H / kT}$$

where m is the electron mass, χ_H is the ionization potential of the hydrogen atom. The population levels are described by the Boltzmann equation. The fraction of atoms at a particular excitation level j will be:

$$\frac{N_j}{N} = \frac{g_j e^{-\epsilon_j/kT}}{u_j}$$

where u_j is the partition function ($u_j = \sum_j g_j e^{\epsilon_j/kT}$), g_j is the statistical weight (the number of states per energy unit), and ϵ_j is the excitation energy at level j above the ground state. The Saha ionization equation and the Boltzmann excitation equation can be combined to find the fraction of atoms in a given ionization or excitation state.

And finally, the net electric charge needs to be zero, i.e.,

$$-N_e + N_p = 0$$

and we will assume no mass loss, and hence the total number particles need to be also conserved:

$$N_{\text{tot}} = N_p + N_e + \sum_i^{nlev} N_i$$

where N_e is the number of electrons, N_p the number of protons, and N_i the number of atoms at level i.

8.1 Opacities

In a white dwarf atmosphere, several absorption processes will determine the opacity of the gas and must be taken into account in solving the radiative transfer equation. Since most white dwarfs are hydrogen-rich, we will consider the absorption processes that can occur in an hydrogen gas.

- Absorption by neutral hydrogen between bound levels (bound-bound), that is between principal quantum numbers $n = l$ (lower level) and $n = u$ (upper level), where the energy of a level is given by $E_n = 13.595 eV/n^2$.

- Absorption by neutral hydrogen between a bound level and the continuum (bound-free), and between two free states (free-free).

- Bound-free and free-free absorption by the negative hydrogen ion (H^-).

- Scattering of light by neutral hydrogen (HI - Rayleigh scattering) and by electrons (e^- - Thomson scattering).

Due to spontaneous decay, energy levels have a finite lifetime, and therefore, a finite energy width $\Gamma_{\text{nat}} = \Delta E_l/h$, which is the natural width of a line expressed in frequency units. Other mechanisms contribute to the broadening of lines, such as:
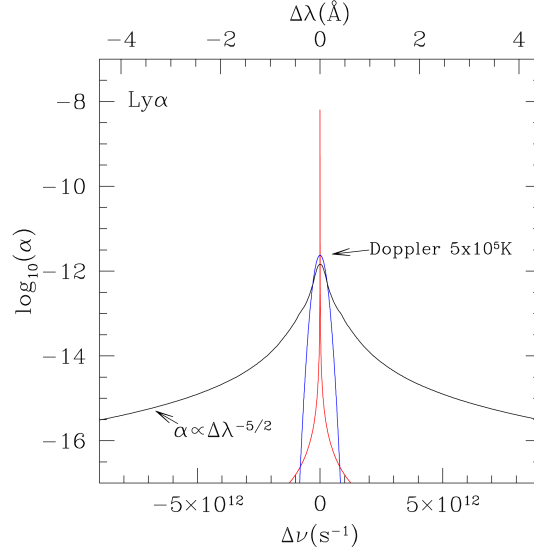
Figure 13: Stark broadening compared to thermal broadening and natural broadening of Lyman α at $T_{\text{eff}} = 50\,000$ K.

- Thermal broadening: each atom has a component of velocity along the line of sight to the star due to its thermal energy. Since there is a distribution of velocities, then the line will be shifted according to the velocity distribution and hence broadening the line.

- Pressure broadening: due to collisional interaction between the atoms absorbing the light and other particles. The collisions, or interactions between particles cause the energy levels of an atom to be perturbed.

- Rotation: if a star is rotating, then the line profile will also be broadened where the lines will be Doppler shifted.

In white dwarf atmospheres, pressure broadening dominates over thermal broadening because of the high-density atmospheres. How much an energy level is perturbed depends on the interacting particles and the separation R between the absorber and the perturbing particle. The upper level is more likely to be affected by any nearby particles, and therefore the upper level will experience the largest perturbation. The change in energy induced by the interactions between particles can be represented by:

$$\frac{\Delta E}{h} = \Delta \nu = \frac{C_n}{R^n}$$

where C_n is the interaction constant and n is the power-law index. Therefore, R^{-n} describes the type of potential the particles are subjected to during an interaction. Some of the interactions that particles can experience are:
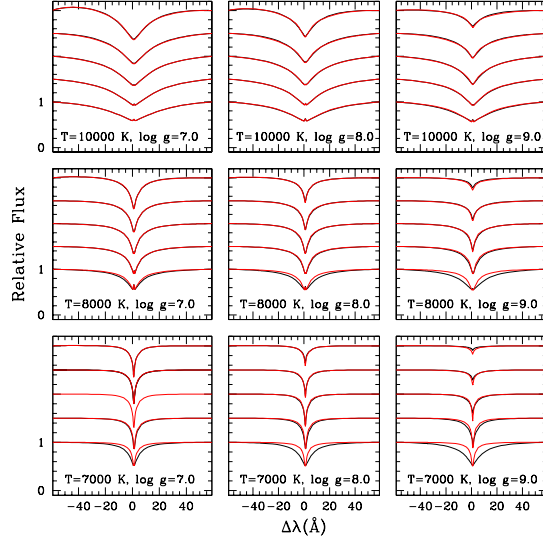
Figure 14: The line profiles of Hα to Hϵ are shown (from bottom to top) for the given temperature and surface gravity. The profiles shown in black include resonance broadening and the profiles in red do not.

- $n = 2$ - Linear Stark effect for hydrogen atoms perturbed by protons and electrons.

- $n = 3$ - Resonance broadening, that is dipole-dipole interactions when the neutral particles are of the same species.

- $n = 4$ - Quadratic Stark effect for most atoms that are perturbed by electrons.

- $n = 6$ - van der Waals broadening, that is dipole-dipole interaction when the neutral particles are of different species.

In white dwarfs, linear Stark broadening affects the hydrogen lines and is dominant in white dwarfs with $T_{\text{eff}} \gtrsim 10\,000$ K, since hydrogen is mostly ionized. Figure 13 shows a comparison of linear Stark broadening to Doppler broadening and natural broadening of Lyman α for a white dwarf at an effective temperature of 50 000 K. It shows that the linear Stark effect is the dominant form of broadening. The number density of electrons and protons in the atmosphere that would produce such a broadening is $n_e = n_p = 10^7$ cm^{-3}.

In cooler white dwarfs ($T_{\text{eff}} \lesssim 10\,000$ K) where hydrogen is mostly neutral, resonance broadening needs to be considered. For an atmosphere which also contains other species of atoms, such as helium, then van der Waals broadening also becomes important. Figure 14 shows the Balmer line profiles for varying temperature and surface gravity. The effect if resonance broadening is shown
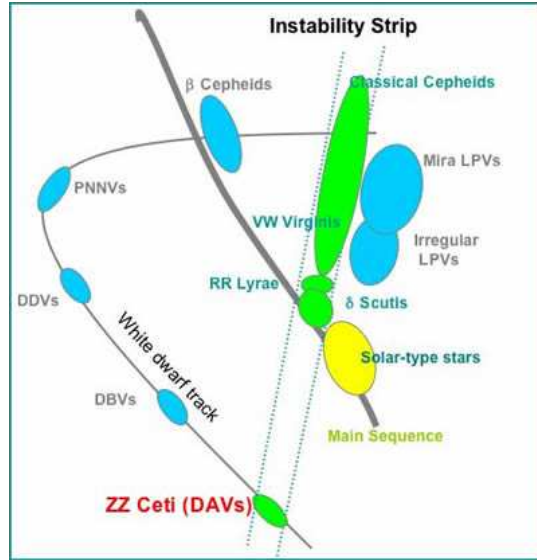
28

Figure 15: Pulsating stars across the Hertzprung-Russell diagram.

by comparing spectral line profiles which include resonance broadening to lines which do not. Resonance broadening becomes prominent at lower temperatures (i.e., $T_{\text{eff}} \leq 8000$ K) where neutral hydrogen atoms are more numerous and more likely to interact with the radiative atoms.

9 Variable White Dwarfs

The first pulsating star to be discovered was Mira (*o* Ceti). David Fabricius observed Mira in August 1595 and then again in October 1595, when it faded from view. He observed Mira to reappear in February 1596. The 11 month period of Mira was not determined until Johann Fokkens Holwarda observed it in 1638. The magnitude of Mira varies between approximately 2nd to 9th magntitude. The second pulsating star was not discovered until 1784, when John Doosricke observed and measured the period (5 days 8 hours 48 minutes) of δ Cephei. This star became the prototype for the pulsating Cepheid stars.

In 1893, Henrietta Swan Leavitt began working at Harvard Observatory for Edward C. Pickering, where she measured and cataloged the brightest stars in the observatory's photographic plates. During this time she discovered many variable stars, in particular in the Magellanic Clouds (Leavitt, 1908). She also noticed that the brighter Cepheids had longer pulsation periods (Leavitt & Pickering, 1912). This relationship allowed Cepheid stars to be used as distance indicators.

The different types of pulsating stars are listed in Table 2 and Figure 15 shows their location on the Hertzprung-Russell diagram. The variability of

Table 2: Types of pulsating stars.

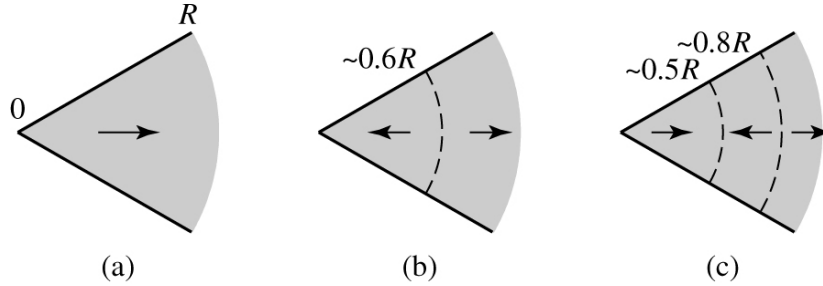| Type	Period	Radial/Non-radial
Long-period variables	100-700 days	R
Classical Cepheids	1-50 days	R
WV Virginis stars	2-45 days	R
RR Lyrae stars	1.5 - 24 hours	R
δ Scutis stars	1-3 hours	R/NR
β Cephei stars	3-7 hours	R/NR
ZZ Ceti stars	100 - 1000 seconds	NR

Figure 16: Standing waves within a star, (a) shows the fundamental mode, (b) 1st harmonic/overtone, (c) 2nd harmonic/overtone.

these stars remained unexplained until 1914, when Harlow Shapley suggested that radial pulsations could explain the observed variability in brightness and temperature (Shapley, 1914).

Radial variations of a pulsating star are the result of sound waves resonating in the star's interior. Infact they are standing waves with the node at the center of the star and the anti-node at the surface. Figure 16 shows how the stars can pulsate in different modes. Most stars pulsate in the fundamental mode, however some stars such as RR Lyrae can pulsate in the 1st harmonic as well. The pulsation period depends on the radius and density of the stellar interior.

In 1918, Arthur Eddington suggested that pulsating stars are thermodynamic heat engines. The gas in the star needs to do $P\ dV$ work as it expands and contracts throughout the pulsation cycle. If the total work is positive, i.e., $\oint P\ dV > 0$, then the oscillations will grow in magnitude, however if the total work done is negative, i.e., $\oint P\ dV < 0$ then the oscillations will decay. The layers will pulsate until an equilibrium value is reached, that is when the total work done is zero. The net work done by each layer of the star during one cycle is the difference between the heat flowing into the gas and the heat leaving the gas. For driving the oscillations, the heat must enter the layer during the high temperature stage of the cycle and leave during the low temperature stage, that is the driving layers of a pulsating star must absorb heat around the time

of their maximum compression. Therefore, maximum pressure will occur after maximum compression and will force the gas to expand and hence causing the oscillations to amplify.

Eddington suggested that stars, the oscillations can be driven by the *valve mechanism*. Therefore for a star to pulsate the layer of the star needs to become more opaque upon compression so that the photons are trapped and as a result heating the gas and increasing the pressure. This high pressured gas then expands and as it becomes more transparent, the photons can escape, allowing the gas to cool and as a result causing the pressure to drop. The gas layer then can fall back down due to gravity. Therefore in this model, the observed variations correspond to the temperature change, the change in radius is has a much smaller effect on the variations of emitted light.

In most stars the opacity increases with greater density. Remember Kramer's opacity law (Eqn. 24):

$$\kappa = \kappa_0 \rho T^{-3.5}.$$

From this equation we can see that the opacity increases as the density increases and temperature decreases. Since the opacity is more sensitive to the temperature ($\kappa \propto T^{-3.5}$) than to the density ($\kappa \propto \rho$) then upon compression the density increases and temperature also increases, and hence the opacity will decrease. This would dampen the any oscillations, and would explain why most stars do not pulsate.

The stars where the valve mechanism can operate are stars that have partial ionization zones. The reason is that within layers of the star where the gas is partially ionized, part of the work done on the gas as it is compressed produces further ionization rather than raising the temperature of the gas. With a smaller temperature increase, the density in Kramer's opacity law can dominate and therefore the opacity will increase. Simalarly, when the gas expands, the temperature does not decrease as much as expected because the ions recombine with electrons and as a result release energy. And again the density term dominates, the opacity will decrease during expansion. This process is called the κ mechanism.

White dwarfs with temperatures around $12\,000$ K have been observed to be variable ($\lesssim 0.2$ magnitudes) with periods between ~ 100 and ~ 1000 seconds. The first variable was discovered by Arlo Landolt in 1968 (Landolt, 1968), who noticed that the *standard* star HL Tau 76 was infact variable. Shortly following this discovery, several searches for other variable white dwarfs were conducted with success. This led to the discovery of ZZ Ceti (Lasker & Hesser, 1971), which has become the proto-type for variable DA white dwarfs. Winget et al. (1982a) showed that the hydrogen partial ionization zone was responsible for driving the oscillations in variable DA white dwarfs. They also predicted that in hotter DB variable white dwarfs should also be observed where the driving mechanism is the helium partial ionization zone. In the same year Winget et al. (1982b) reported the discovery of the variable DB white dwarf, GD 358. Since this discovery, several more variable DB white dwarfs have been discovered, as well as a small number of variable DO white dwarfs (also known as PG1159

Table 3: Variable White Dwarfs

Type	Temperature (K)	Driving mechanism
ZZ Ceti stars (DAV)	$\sim 10\,500 - 13\,000$	H-partial ionization zone
DBV	$\sim 22\,000 - 27\,000$	He-partial ionization zone
PG1159 stars (DOV)	$\sim 80\,000 - 140\,000$	

stars). Table 3 summarizes the properties of the three groups of variable white dwarfs.

Up to now, radial pulsations have been assumed to operate within stars, and imagined the star to vary radially. However, in variable white dwarfs non-radial oscillations are observed. The non-radial oscillations can be described by three different modes:

- p-modes, where pressure provides the restoring force, and can be both radial and non-radial.

- g-mode, where gravity provides the restoring force, and only displayes non-radial modes of oscillations. These oscillations are connected to the buoyancy and convection within the stellar atmosphere.

- f-mode, imtermediate between p- and g-modes, and only displays non-radial modes of oscillations.

The spherical symmetry of white dwarfs allow the stellar pulsations to be described using spherical harmonic functions. Each pulsation mode can be described by 3 integer numbers (similarly to the quantum mechanical wave function of an H atom). These numbers are:

- k or n: determines the number of times the surface oscillates between the center of the star and the surface. This behaviour is hidden deep below the visible surface, however k can be determined from the pulsation period. A lower value of k means a shorter period.

- l: determines the number of borders between the hot and cold zones on the stellar surface.

- m: represents the number of borders between the hot and cold zones on the stellar surface that pass through the pole of the star's rotation axis. The values of m are limited to $-l \leq m \leq l$.

10   White Dwarf Luminosity Function

White dwarfs are useful in helping to determine the age of the Galactic disk or stellar clusters.

A white dwarf luminosity function is the number of stars per luminosity bin. When determining the luminosity function, the volume of space sampled needs to taken into account.

References

Adams, W.S. 1914, PASP, 26, 198

Adams, W.S. 1915, PASP, 27, 236

Adams, W.S. 1925, Proc. N.A.S., 11, 382

Barstow, M.A., Bond, H.E., Holberg, J.B., Burleigh, M.R., Hubeny, I., & Koester, D. 2005, MNRAS, 362, 1134

Benvenuto, O.G. & Althaus, L.G. 1999, MNRAS, 303, 30

Bergeron, P., Saffer, R.A., & Liebert, J. 1992, ApJ, 394, 228

Bessel, F.W. 1844, MNRAS, 6,136

Cannon & Pickering, 1918, Harvard Annals, 92

Chandrasekhar, S. 1935, MNRAS, 95, 207

Christlieb, N., Wisotzki, L., Reimers, D., Homeier, D., Koester, D., & Heber, U. 2001, A&A, 366, 898

Eddington, A.S. 1924, MNRAS, 84, 308

Finley, D.S. & Koester, D. 1997, ApJ, 489, L79

Fowler, R.H. 1926, MNRAS, 87, 114

Giclas, H.L., Burnham Jr., R., & Thomas, N.G. 1971, Lowell Proper Motion Survey: 8991 Northern Stars, Lowell Obs.

Giclas, H.L., Burnham Jr., R., & Thomas, N.G. 1978, Lowell Proper Motion Survey: Southern Hemisphere Catalog, Lowell Obs. Bull. No. 164

Green, R.F., Schmidt, M., & Liebert, J. 1986, ApJS, 61, 305

Greenstein, J.L., Oke, J.B., & Shipman, H.L. 1971, ApJ, 169, 563

Holberg, J.B., Barstow, M.A., & Burleigh, M.R. 2003, ApJS, 147, 145

Kawka, A., Vennes, S., Schmidt, G.D., Wickramasinghe, D.T., & Koch, R. 2006, ApJ, 654, in press

Kilkenny, D., O'Donoghue, D., Koen, C., Stobie, R.S., & Chen, A. 1997, MNRAS, 287, 867

Kuiper, G.P. 1941, PASP, 53, 248

Lamontagne, R., Demers, S., Wesemael, F., Fontaine, G., & Irwin, M.J. 2000, AJ, 119, 241

Landolt, A.U. 1968, ApJ, 153, 151

Lasker, B.M. & Hesser, J.E. 1971, ApJ, 163, L89

Leavitt, H.S. 1908, Annals of Harvard College Observatory, 60, 87

Leavitt, H.S. & Pickering, E.C. 1912, Harvard College Observatory Circulars, 173, 1

Marsh, M.C., Barstow, M.A., Buckley, D.A., Burleigh, M.R., Holberg, J.B., Koester, D., O'Donoghue, D., Penny, A.J., & Sansom, A.E. 1997, MNRAS, 286, 369

Mestel, L. 1952, MNRAS, 112, 583

Russell, H.N. 1913, The Observatory, 36, 324

Russell, H.N. 1914, Nature, 93

Salim, S. & Gould, A. 2002, ApJ, 575, L83

Sion, E.M., Greenstein, J.L., Landstreet, J.D., Liebert, J., Shipman, H.L., & Wegner, G.A. 1983, ApJ, 269, 253

Shapley, H. 1914, ApJ, 40, 448

van Maanen, A. 1917, PASP, 29, 258

Vennes, S. 1999, ApJ, 525, 995

Vennes, S., Thejll, P.A., Génova-Galvan, R., & Dupuis, J. 1997, ApJ, 480, 714

Vennes, S., Thejll, P.A., Wickramasinghe, D.T., Bessell, M.S. 1996, ApJ, 467, 782

Wesemael, F. 1985, QJRAS, 26, 273

Winget, D.E., Robinson, E.L., Nather, R.E., & Fontaine, G. 1982b, ApJ, 262, L11

Winget, D.E., Van Horn, H.M., Tassoul, M. Hansen, C.J., Fontaine, G., & Carroll, B.W. 1982a, ApJ, 252, L65

Wolff, B., Jordan, S., & Koester, D. 1996, A&A, 307, 149

Wood, M.A. 1995, in White Dwarfs, ed. D. Koester & K. Werner (New York: Springer), 41

11 Additional Reading

- Gray, D.F. *The observation and analysis of stellar photospheres*, 1992, Cambridge University Press

- Clayton, D.D. *Principles of Stellar Evolution and Nucleosynthesis*, 1983, University of Chicago Press

- Bradley, W.C. & Ostlie, D.A. *An Introduction to Modern Stellar Astrophysics*, 2006, Addison Wesley Publishing Company, 2nd ed.

- Rose, W.K. *Advanced Stellar Astrophysics*, 1998, Cambridge University Press